


Ultrahigh-Resolution Direct-Frequency-Comb Spectrometer

Faisal Karim¹,* Sarah K. Scholten¹, Christopher Perrella¹, and Andre N. Luiten¹
*Institute for Photonics and Advanced Sensing (IPAS), The University of Adelaide, Adelaide,
South Australia 5005, Australia*

 (Received 15 January 2020; revised 22 June 2020; accepted 20 July 2020; published 28 August 2020)

At low pressures, molecular spectra typically exhibit a large number of very narrow absorption features spread across a relatively wide spectral bandwidth. In order to obtain an accurate estimate of the line shapes, widths, and depths of these absorption features it is a requirement that one performs spectroscopy that is both densely spaced and high resolution across the entire spectral range. Here we demonstrate an approach that delivers on this need: it makes use of an optical frequency comb as the light source along with an optical filter cavity and a dispersive spectrometer to acquire high-resolution spectra with dense spectral sampling. The technique has the potential to acquire spectra with a resolution limit imposed solely by the frequency stability of the comb. As a proof of concept we measure the absorption spectrum of acetylene with a 7.86-MHz spectral spacing over 3.4-THz (25 nm) spectral range. This represents more than 430 000 individual spectral measurements, which are each individually free from the instrumentation broadening that limits conventional spectrometers. Using this spectrum, we extract the thermodynamic properties (temperature, pressure, and molecular density) of the gas sample with high accuracy and precision while simultaneously performing gas compositional analysis.

DOI: [10.1103/PhysRevApplied.14.024087](https://doi.org/10.1103/PhysRevApplied.14.024087)

I. INTRODUCTION

High-resolution broadband spectroscopy of molecules is vital for performing analytic gas measurements, yielding essential information on material structure for physical, chemical, and biological sciences [1]. Each molecule has a unique set of rotational-vibrational transitions that possess a well-defined shape and finite widths, which can be used to identify molecules precisely and accurately, known as molecular fingerprinting [2]. The retrieval of these rovibrational transitions with correct line shapes and strengths is extremely important for understanding fundamental molecular physics (e.g., line-shape models) and atmospheric physics [3,4]. In addition it can be used for studying energy-level structure of molecules and their thermodynamics properties such as elastic and inelastic collisions [2,5]. Retrieval of correct line shapes with accurate depths, widths and positions allows for extraction of spectroscopic parameters such as temperature, pressure, and density of molecules in a sample with high accuracy and precision. As the width of the spectral features can be quite narrow, ranging from kHz to MHz, this necessitates the need for developing a high-resolution spectroscopic technique with dense spectral sampling to aid in unraveling and studying these complex molecular spectra over a broad spectral bandwidth.

An alternative tool for probing molecular systems is the optical frequency comb (OFC), which has enabled real-time detection [6] and identification of gases in mixtures [7] including applications in the oil and gas industry [8], environmental monitoring [9], and breath analysis [10]. OFCs can be near-ideal interrogation sources in these types of applications as they deliver light in a large number of closely spaced and bright sources that are spread over a broad spectral bandwidth. When combined with the high spectral and spatial coherence of OFCs this can enable precise, high-resolution spectroscopy with absolute frequency accuracy [11–14].

Thus, the development of broadband and high-resolution OFC-based spectrometer systems has been the subject of intense interest over recent years [14–16]. Approaches to OFC spectroscopy have taken various routes including direct frequency-comb spectroscopy (DFCS) [11,14,16–18], Fourier transform spectroscopy [19,20], cavity ring-down spectroscopy [10], dual-comb spectroscopy [13,21,22], and single-comb heterodyning techniques [5]. A key decision in any OFC spectrometer is the technique that is used to unravel a comb into its component frequencies. DFCS offers one of the simplest approaches where the OFC itself is used to interrogate a sample, and then the incident and transmitted combs are spatially dispersed onto an optical detector [11,23]. The ratio of these two measurements then yields the transmittance of the sample. One particular approach, that we use here, uses a virtually imaged phased array (VIPA) as

*faisal.karim@adelaide.edu.au

the high-resolution dispersive element. This technique has the ability to generate high-resolution spectra over tens of nanometers of bandwidth [2,11,17,18,24].

Before addressing the technique used in this paper, it is important to remark that in most conventional spectrometers little effort has been taken to differentiate between the concept of spectral sampling (i.e., the frequency separation between adjacent measurements of the transmittance) and the concept of spectral resolution (i.e., the minimum frequency separation between two transmittance measurements that are independently measurable). One imagines that this approach has arisen because, with conventional spectrometers, the logical frequency sampling interval is chosen to be at, or above, the spectral resolution of the instrument, which is, in turn, set by some inherent instrumentation broadening [25]. However, in a carefully designed OFC-based spectrometer these two concepts can have a radically different value: the frequency sampling is set by the effective frequency spacing of the comb modes, whereas the spectral resolution is set by the frequency stability of the frequency comb modes.

In a typical OFC spectrometer, it is the case that the spectral resolution of the VIPA is poorer than the spacing between the comb modes, and in that scenario, the spectrometer is much like a conventional white-light spectrometer where the effective spectral resolution is set by the instrumentation broadening imposed by the VIPA. On the other hand, if one attains a situation where the VIPA resolution is significantly higher than the comb spacing, so that each mode can be resolved, then in this case the instrumentation broadening (and thus the spectral resolution) can be instead set by the frequency instability of the comb modes themselves. We have demonstrated this previously [26] although that was achieved by generating a comb with a very wide spacing between modes. Unfortunately, that approach to high spectral resolution comes at the expense of a relatively poor spectral sampling.

In contrast, here we demonstrate a technique to deliver high spectral sampling while maintaining excellent spectral resolution. Here, we use an approach similar to one developed in 2007 [11], where we still optically filter the frequency comb so that the comb is sufficiently spectrally sparse so that the VIPA is able to resolve the individual modes. However, we then step the repetition rate of the comb, and simultaneously tune the optical filter cavity, so that we obtain a new independent set of transmittance measurements of the gas under study. In this case, we can choose an arbitrarily dense spectral sampling through control of the repetition rate, while also avoiding any unwanted broadening effects of the VIPA spectrometer.

We demonstrate the power of our technique by performing spectroscopy on a low-pressure sample of acetylene (C_2H_2) at 1525 nm with a spectral sampling of 7.86 MHz spanning 3.4 THz (25 nm) of spectral bandwidth. The measured absorption spectrum agrees very favorably with

a model spectrum based on parameters from the high-resolution transmission molecular absorption (HITRAN) database [27]. In addition, the obtained spectrum displays no instrumentation broadening at the spectrometer output.

We note the recent reporting of some work [14,15] that has some overlap with the work reported here. In that work, the authors demonstrated a very high sampling density of an enhancement cavity transmission function in order to measure the effect of the gas on the cavity. However, the effective spectral sampling of the gas itself in both cases was at the level of 1 GHz. The approach used in this paper effectively samples the gas transmittance with a density that is 100 times higher than those previous reports—this is particularly useful for interrogating low-pressure gases where the spectral features themselves are very narrow.

With our high-resolution technique, we show complete gas characterization by successfully measuring the gas thermodynamic properties (i.e., temperature, pressure, and molecular density) with high accuracy and precision while simultaneously performing gas compositional analysis. We believe our technique is a useful tool for physicists and spectroscopists to study complex molecular spectra.

II. EXPERIMENTAL METHODS

A. Optical experiment

An optical frequency comb delivers up to hundreds of thousands of individual frequency modes in a single beam of light. The absolute frequency of each comb mode is given by the following equation:

$$f_n = nf_r + f_0, \quad (1)$$

where n is a large positive integer (approximately 786 341 in our case), and f_0 is the carrier-envelope offset frequency (20 MHz in this experiment) [12]. The spacing between these modes is known as the comb's repetition rate (f_r), which is typically below the resolution of a dispersive spectrometer [7,28]. Since each mode carries vital information about the sample, this poses a significant challenge in being able to obtain all of the potential information in a comb-based measurement. To overcome this challenge, we optically filter the comb so that the modes are now sufficiently sparse to be easily resolved by the spectrometer. This is achieved by using a length-stabilized low-finesse (approximately 200) Fabry-Perot (FP) cavity that rarefies the OFC by allowing only every 36th comb mode to pass through. The repetition rate of the filtered comb is then $36 \times f_r \approx 9$ GHz (with $f_r = 250$ MHz), which is sufficiently sparse for modes to be resolved individually by a highly dispersive spectrometer [11,24,26]. However, a byproduct of this approach is the limiting of spectral sampling to 9 GHz, or to 250 MHz as in Ref. [26] by tuning the FP cavity length. This means a substantial loss of spectral

information, especially for molecules that possess narrow absorption features of hundreds of MHz to GHz scales.

In this paper we overcome the sparse sampling challenge by stepping the frequency comb and tuning the FP optical cavity simultaneously. In particular, we tune f_r in small steps of $\Delta f_r = 10$ Hz. The gas is then sampled by a rarefied comb with an effective repetition rate of $f_{r \text{ eff } m} = 36 \times (f_r + m\Delta f_r)$, which samples a different subset of the molecular spectrum each time f_r is stepped by Δf_r , where $m = 0, 1, 2, \dots, 1145$ covers one free spectral range of the filtering FP cavity. The rarefied comb modes have frequencies given by Eq. (1), where f_r is replaced by $f_{r \text{ eff } m}$, and n is replaced by $n_{\text{eff}} = n/36$. This gives us the rarefied absolute frequency of each comb mode at the m th repetition rate step to be

$$\begin{aligned} f_{n,m} &= n_{\text{eff}} f_{r \text{ eff } m} + f_0, \\ f_{n,m} &= n_{\text{eff}} 36 \times (f_r + m\Delta f_r) + f_0. \end{aligned} \quad (2)$$

This technique is illustrated in Fig. 1. The FP cavity automatically tracks the shifted comb modes by varying its length to maintain the resonance condition throughout the experiment [26]. The step size, Δf_r , determines the sampling resolution of the transmission spectrum, which can be set arbitrarily. For the proof of principle displayed in this paper, the choice of $\Delta f_r = 10$ Hz results in the optical comb modes shifting by $\Delta f_{n,m} = f_{n,m+1} - f_{n,m} = 7.86$ MHz.

The experimental setup we use to demonstrate this technique is shown in Fig. 2. An OFC (Menlo Systems FC1500) is used as the sample interrogation source, which spans 1500–1700 nm and has a repetition rate of 250 MHz

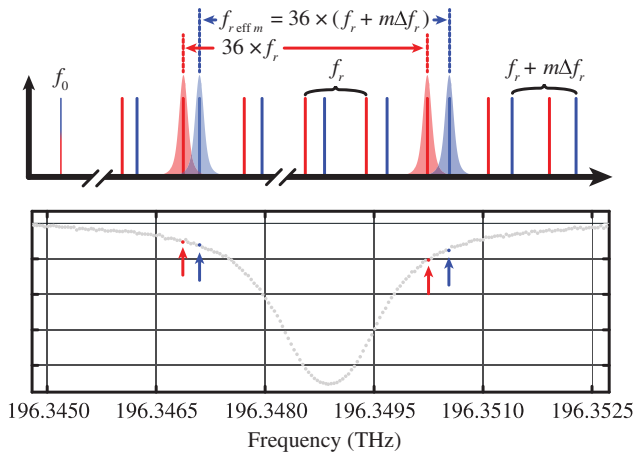


FIG. 1. Illustration of the comb rarefaction and interleaving technique. The original comb subset with mode spacing $36 \times f_r$ is shown in red, while a new comb subset (blue) with an effective repetition rate $f_{r \text{ eff } m} = 36 \times (f_r + m\Delta f_r)$ is obtained by shifting the repetition rate by m increments of Δf_r . The sampling of the spectrum is shown in corresponding colors.

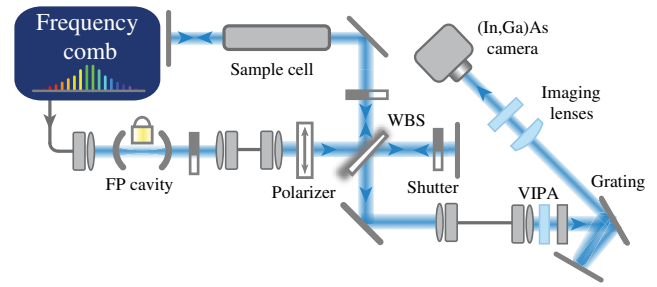


FIG. 2. Diagram of the experimental setup for high-resolution spectroscopy of acetylene. Blue, free-space path of the optical frequency comb; gray, optical fibres; FP, Fabry-Perot (cavity); WBS, wedged beam splitter.

that can be tuned by ± 2.6 MHz. Both f_r and the carrier-envelope offset frequency (f_0) are stabilized to a Caesium beam clock (Datum CsIII).

The filtered comb is first passed through a polarizer before being split into the reference and sample paths via a 50:50 wedged beam splitter (WBS). The reference arm is used to measure the incident spectrum while the sample arm contains a double-passed 5-cm C_2H_2 gas cell (50 ± 5 Torr, Wavelength References) at room temperature. Each path is equipped with a computer-controlled shutter that allows switching between paths. The return beams from both paths are then sent to the spectrometer via an optical fiber to ensure collinearity at the spectrometer input.

The spectrometer is based upon a VIPA etalon that disperses the beam as a function of frequency [29]. Light from the reference and sample path is first directed through a cylindrical lens, which line focuses the light into the antireflective-coated input window of the VIPA. The VIPA then disperses the beam vertically and has a free spectral range (FSR) of approximately 50 GHz and finesse of approximately 100. When used in isolation the VIPA suffers from a frequency ambiguity, sending frequencies separated by multiples of the VIPA FSR to the same spatial location. To remove this ambiguity, a 600 lines/mm diffraction grating is used to spectrally disperse the overlapped modes in the orthogonal direction, producing a two-dimensional (2D) array of fully resolved comb modes (dot pattern) when the filtered comb is incident on the spectrometer [11]. The grating is double passed to improve horizontal angular resolution and to minimize any crosstalk between adjacent VIPA stripes. The 2D array of comb modes are then focused onto and imaged by an (In, Ga)As camera (Xenics XEVA-1.7-320) [12]. A typical filtered-comb sample-path image is shown in Fig. 3 in which modes that get absorbed by the sample appear missing, highlighted with green arrows, while the black dots represent transmitted modes. Each image spans 3.4 THz (25 nm) of spectral range in the horizontal direction, limited by the camera field of view, and just over one VIPA FSR in the vertical direction.

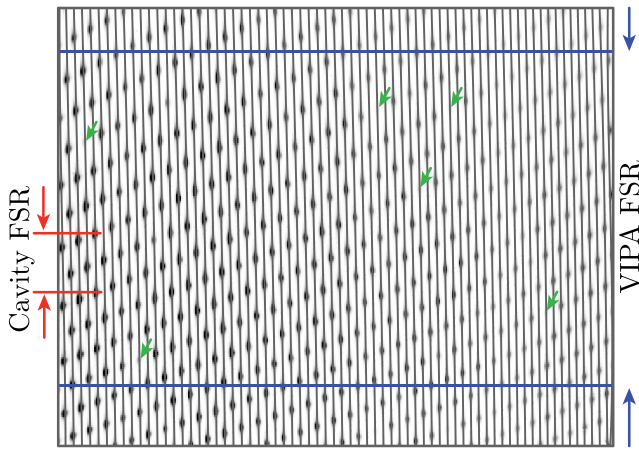


FIG. 3. A typical sample path image showing the rarefied comb (inverted colors). The blue horizontal lines mark one VIPA FSR containing unique spectral data, while the red horizontal lines denote one cavity FSR of $36 \times f_r$. The horizontal separation of adjacent vertical stripes with the centers as mapped from a filtered image (overlaid in light gray stripes) is also one VIPA FSR. There are typically five to six cavity-filtered comb modes per vertical VIPA stripe. Several comb modes are absorbed by acetylene (green arrows).

B. Image analysis

A set of four images are taken at each repetition rate using the optical shutters: bright images of reference and sample paths illuminated by the OFC followed by dark images of the same paths with matching camera integration time. The dark images are subtracted from their corresponding bright images to remove camera dark backgrounds or any background light. The resulting images are then corrected for camera nonlinearity on a pixel-by-pixel basis, based on previously obtained gray images [30]. Using a reference path image, mode centers are located and the total power of each mode is calculated for both reference and signal-path images. As the mode is asymmetrical in shape and illuminates more than one pixel on the camera, the optical power is summed over multiple pixels defined by a box of 13 high \times 5 wide pixels. The size of the box is chosen such that maximum power is captured while keeping enough buffer zone for any light spillage from nearby modes. The power in each mode of the signal-path image is then ratioed with the corresponding power in the reference-path image to yield a filtered transmission spectrum with approximately 9-GHz frequency spacing for a particular effective repetition rate.

A complete densely sampled C_2H_2 spectrum is created by combining the results of the individual filtered spectra that are taken by moving the repetition rate of the comb to 1145 equally spaced values. To improve the SNR of the final spectrum, 20 spectra are acquired at each repetition rate, and these are averaged together. The details of the

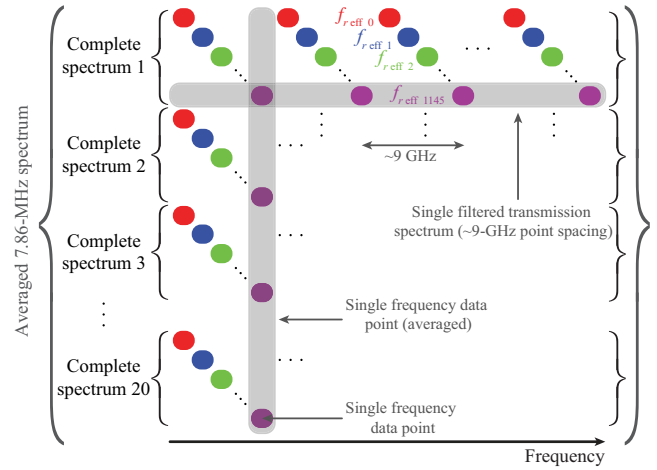


FIG. 4. Spectral interleaving and averaging for generation of error bars and improved spectral SNR. For each value of effective repetition rate $f_r^{\text{eff } m} = 36 \times (f_r + m\Delta f_r)$ (colors), a filtered spectrum is generated with a single frequency data point every cavity FSR (9 GHz) (horizontal gray box). By interleaving filtered spectra for all values of $m = 0, 1, 2, \dots, 1145$ one produces a single complete densely sampled spectrum (small braces). Overall, 20 such spectra are averaged together at each frequency data point (vertical gray box) to produce the final averaged 7.86-MHz sampled spectrum shown in Fig. 5 (large braces). Each complete densely sampled spectrum is fitted individually to produce 20 sets of fitting values for error-analysis purposes as explained in the main text.

spectral interleaving and averaging processes are shown in Fig. 4.

This repeated measurement also allows us to estimate the precision of the transmittance measurement, as described later in the results section.

An absolute frequency axis is derived from Eq. (1) using the comb's repetition rate (f_r) and the carrier-envelope offset frequency (f_0) that are measured at each repetition rate step. Using the knowledge of the VIPA FSR and cavity FSR, we can derive a value, n , for the absolute mode number by comparing the obtained spectrum to the absorption frequencies as listed in the HITRAN database [27].

III. RESULTS

Figure 5 displays the resulting averaged transmission spectrum with 7.86-MHz spectral sampling, containing approximately 430 000 data points spanning over 3.4 THz (25 nm) of spectral bandwidth. The obtained molecular spectra is free of instrumentation broadening from the spectrometer readout, thereby overcoming the 2-GHz resolution limit imposed by the VIPA spectrometer [31]. We demonstrate the ultrahigh spectral resolution of our approach in Fig. 6—here we show a portion of the averaged 7.86-MHz-sampled spectrum (from Fig. 5) in comparison with one obtained under the same conditions but where we do not pass the comb through the filtering

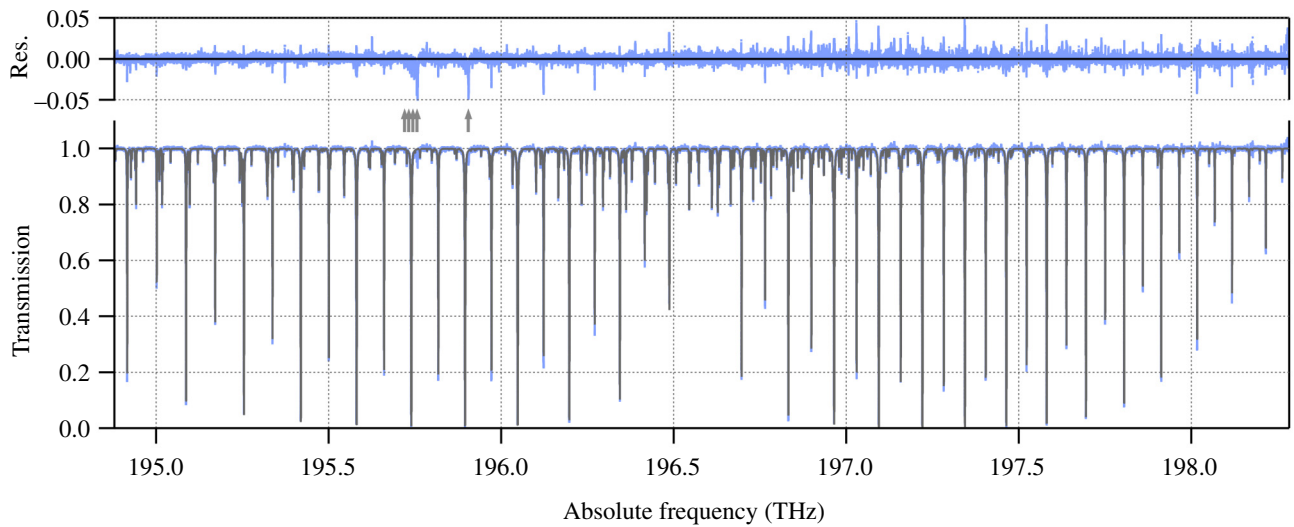


FIG. 5. High-resolution averaged acetylene spectrum (blue markers) with fit results using parameters from the HITRAN database (gray solid line) for both $^{12}\text{C}_2\text{H}_2$ and $\text{H}^{12}\text{C}^{13}\text{CH}$. Some unfitted rovibrational transitions appear in the residuals (gray arrow markers) [27] while the rest of the structures are poorly fitted residuals.

optical cavity. In that case the spectral resolution of the VIPA intervenes to create instrumental broadening. We also show a theoretical spectral model, which includes the influence of Doppler and pressure broadenings on the line shape. It can be seen that in the case of the unfiltered frequency comb, instrumentation broadening severely affects the widths and depths of transitions, along with merging and smearing of adjacent small peaks. A very good model, or measurement, of the instrumental broadening allows for some correction of this unwanted influence, but it is frequently the case that this broadening can be both frequency dependent and nonanalytic, which can challenge high-quality correction.

One may now ask what sets the effective spectral resolution of the frequency spectrometer in the case where each of the comb modes has been fully resolved by the VIPA. We suggest that in this case the relevant measure is the frequency fluctuations of the frequency comb modes that occur during the measurement. The repetition rate of the comb is locked to a frequency synthesizer that is referenced to a Cs beam clock. This results in measured frequency fluctuations of the optical modes of approximately $80 (\pm 12)$ kHz. Of course, this could be much improved by frequency locking an individual mode to a high-quality optical frequency standard to deliver frequency instability at the Hz level [32–34].

The final averaged 7.86-MHz-sampled spectrum is acquired over approximately 5 h. We note some slow drifts that occur over this period in the relative power split at the 50:50 splitter, which are corrected by examining the transmittance at a selection of frequency locations at which there is no absorption in the sample. An additional linear background slope, due to a frequency-dependent splitting

factor, is corrected by fitting to the resulting transmittance and dividing it out of the final averaged spectrum.

The absorption bands of $^{12}\text{C}_2\text{H}_2$ and $\text{H}^{12}\text{C}^{13}\text{CH}$ falling within the measured spectral range are simultaneously fitted with a model derived from parameters available on the HITRAN database using a Voigt line shape for the

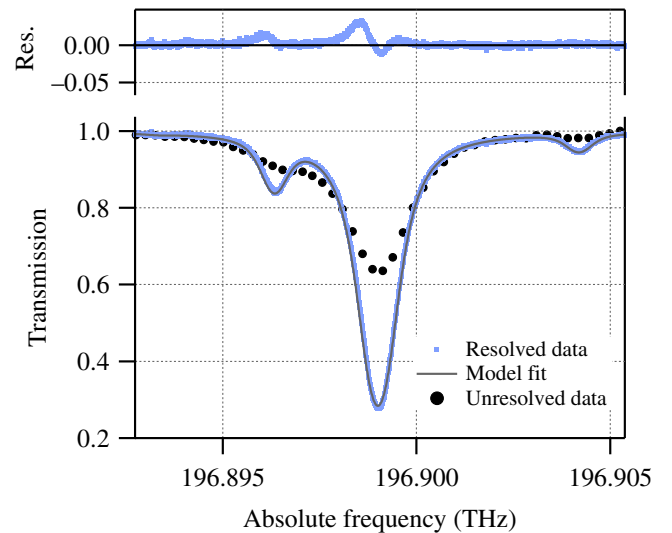


FIG. 6. Enlarged portion of the averaged 7.86-MHz spectrum shown in Fig. 5 (blue markers) with corresponding HITRAN fit (solid gray) and residuals. A spectrum acquired under the same conditions for the unresolved case is shown in black, with the effects of instrumentation broadening apparent [31]. Use of a Voigt line shape during fitting results in structure in the residuals and an underestimate of line strengths [36–39]. Asymmetry of the residuals is likely in part due to an average pressure-shift value being used due to data unavailability [35].

individual absorption features [31]. The model comprised 828 and 40 individual rovibrational transitions of $^{12}\text{C}_2\text{H}_2$ and $\text{H}^{12}\text{C}^{13}\text{CH}$, respectively, the line centers of which are corrected with an average self-pressure-induced line shift [35]. In addition, the Doppler full width at half maximum for each transition, calculated individually, is also included in the fit. Only four parameters are left free in the model—the gas temperature and pressure, as well as the density of the two most abundant isotopes of acetylene.

The model is applied to the final averaged acetylene spectrum, where by analyzing the rotational-vibrational transitions, absorption depths, collisional line broadening, and Boltzmann population distribution, a gas temperature of 23.80(3) °C and pressure of 53.73(1) Torr is extracted, which is in agreement with known laboratory conditions and manufacturing tolerances for the cell. The molecular density of $^{12}\text{C}_2\text{H}_2$ and $\text{H}^{12}\text{C}^{13}\text{CH}$ is found to be $1.715\,56(7) \times 10^{18}$ molecules/cm³ and $3.965(2) \times 10^{16}$ molecules/cm³ from which we can obtain a measured isotopic ratio of 2.311(1)%. This is in reasonable agreement (3%) with the 2.24693% natural abundance ratio of acetylene given in the HITRAN database [27]. The individual isotopic molecular concentrations are also in agreement with expectations for a 50(5) Torr cell at room temperature using the HITRAN database [27].

To obtain error bars for the temperature, pressure, and individual molecular isotopic concentrations, each of the 20 complete densely sampled spectra (as shown in Fig. 4) are fitted with the spectroscopic model, returning 20 values for each fit parameter. The standard error in the mean of these 20 sets of four fit parameters are calculated, which produces the quoted error bounds. These errors represent an estimate of the precision of the measurements. The mean values are the result of fitting the averaged spectrum.

The residuals in Fig. 5 show a few features, marked by gray arrows, which we associate with a small number of unfitted transitions that are not present in the current edition of HITRAN [27]. The sensitivity limit is set by dark noise from the (In, Ga)As camera, which equally affects the four images that contribute to forming a single transmission measurement. This noise is white and thus can be reduced further by averaging a number of independent measurements. Overall, 20 spectra are acquired at each repetition rate, which are averaged together totaling 2 s of camera exposure, resulting in a sensitivity of 1%, or a SNR of 100.

IV. DISCUSSION

Our method enables measurements of spectra with approximately 80-kHz resolution as well as dense spectral sampling of 7.86 MHz using a single frequency comb. Our previous approach to eliminating instrumental broadening, and hence obtaining a high resolution, led to a relatively wide spectral sampling set by the comb's repetition rate of

250 MHz [26]. The 7.86-MHz spectral sampling reported here is chosen as a compromise between acquisition time and dense spectral sampling but is easily varied by the user.

The final spectrum takes 5 h to acquire. The majority of this time is imposed by the relatively slow coarse tuning of the repetition rate of the frequency comb: we find it is necessary to wait for approximately 13 s between changes of the repetition rate in order to ensure that its locking system is reliable. This waiting time is further extended because we directly measure the repetition rate to ensure that it acquires the commanded value—this takes an additional 1 s for each repetition-rate value. The entire measurement duration at a particular repetition rate is 2 s, including the requirement to take four images to obtain a calibrated transmission value and repeating this 20 times to lower the noise of measurement (individual image exposures are around 25 ms). We note that an improved repetition-rate tuning system could reduce the wait time between samples by an order of magnitude leading to a measurement time of 36 min.

The reported technique acquires approximately 100 times denser frequency sampling than that of two recently reported approaches [14,15], while the effective frequency resolution of all three approaches is at the level of tens of kHz. In comparison, dual-comb spectroscopy (DCS) can produce kHz-level resolution [40] but can suffer from low spectral sampling (hundreds of MHz) if the repetition rates of the two combs are fixed. It is possible to tune the repetition rate of one of the combs in DCS and this has been shown to deliver MHz-level spectral sampling, although the process requires stringent frequency control [21,41].

In contrast, a scanning cw laser may also cover 3.4 THz of spectral bandwidth, however being a single frequency source, it can only perform a single absorption measurement at any one time. Whereas an OFC, having thousands of frequencies present simultaneously in a single beam, is capable of performing multiple absorption measurements in parallel. Furthermore, an OFC that is referenced to a frequency standard has inherent absolute accuracy and high precision in the frequency of its absorption measurements, producing spectra with consequent high precision and absolute frequency accuracy.

Our approach offers simplicity and a high-resolution spectrum using just a single frequency comb—this is crucial to obtain accurate values for transition line centers, line shapes, and absorption depths that can yield gas parameters such as pressure, temperature, and concentration of molecules [42,43].

V. CONCLUSION

We demonstrate a method that acquires an approximately 80-kHz resolution spectra with 7.86-MHz spectral sampling and zero instrumentation broadening at the spectrometer readout. The method is based on direct

frequency-comb spectroscopy based around a single tunable frequency comb in conjunction with an optical filter cavity and a VIPA spectrometer. The resolution we demonstrate here is similar to that achievable with the very best of techniques but offers higher sampling resolution and simpler experimental requirements. Our high-resolution spectroscopy technique makes extremely precise and accurate measurements of the thermodynamic properties of a gas while simultaneously performing a compositional analysis for complete gas characterization. We believe our high-resolution spectroscopic technique is a useful tool for physicists and spectroscopists to unravel and study complex molecular spectra.

ACKNOWLEDGMENTS

This work is supported by Australian Research Council (ARC) Linkage Project Grants (LP120200605, LP140100647); IC150100019 as part of the ARC Industrial Transformation and Training Centre for LNG Futures; and the Government of South Australia (The Premiers Science and Research Fund). We thank Dr Nicolas Bourbeau Hébert for his very useful insights on this paper.

F.K. and S.K.S. contributed equally to this work.

-
- [1] S. Kinugawa and H. Sasada, Wavenumber measurement of the 1.5- μm band of acetylene by semiconductor laser spectrometer, *Jpn. J. Appl. Phys* **29**, 611 (1990).
- [2] F. Adler, M. J. Thorpe, K. C. Cossel, and J. Ye, Cavity-enhanced direct frequency comb spectroscopy: Technology and applications, *Ann. Rev. Anal. Chem.* **3**, 175 (2010).
- [3] P. Drossart, B. Bézard, S. Atreya, J. Lacy, E. Serabyn, A. Tokunaga, and T. Encrenaz, Enhanced acetylene emission near the north pole of jupiter, *Icarus* **66**, 610 (1986).
- [4] M. J. Cich, C. P. McRaven, G. V. Lopez, T. J. Sears, D. Hurtmans, and A. W. Mantz, Temperature-dependent pressure broadened line shape measurements in the $\nu_1 + \nu_3$ band of acetylene using a diode laser referenced to a frequency comb, *Appl. Phys. B* **109**, 373 (2012).
- [5] T. Shioda, K. Fujii, K. Kashiwagi, and T. Kurokawa, High-resolution spectroscopy using interleaved 100 GHz optical frequency comb scanned by phase modulator, *Opt. Commun.* **284**, 5180 (2011).
- [6] P. Weibring, D. Richter, J. G. Walega, and A. Fried, First demonstration of a high performance difference frequency spectrometer on airborne platforms, *Opt. Express* **15**, 13476 (2007).
- [7] L. Nugent-Glandorf, T. Neely, F. Adler, A. J. Fleisher, K. C. Cossel, B. Bjork, T. Dinneen, J. Ye, and S. A. Diddams, Mid-infrared virtually imaged phased array spectrometer for rapid and broadband trace gas detection, *Opt. Lett.* **37**, 3285 (2012).
- [8] S. Coburn, C. B. Alden, R. Wright, K. Cossel, E. Baumann, G.-W. Truong, F. Giorgetta, C. Sweeney, N. R. Newbury, K. Prasad, I. Coddington, and G. B. Rieker, Regional trace-gas source attribution using a field-deployed dual frequency comb spectrometer, *Optica* **5**, 320 (2018).
- [9] G. B. Rieker, F. R. Giorgetta, W. C. Swann, J. Kofler, A. M. Zolot, L. C. Sinclair, E. Baumann, C. Cromer, G. Petron, C. Sweeney, P. P. Tans, I. Coddington, and N. R. Newbury, Frequency-comb-based remote sensing of greenhouse gases over kilometer air paths, *Optica* **1**, 290 (2014).
- [10] M. J. Thorpe, K. D. Moll, R. J. Jones, B. Safdi, and J. Ye, Broadband cavity ringdown spectroscopy for sensitive and rapid molecular detection, *Science* **311**, 1595 (2006).
- [11] S. A. Diddams, L. Hollberg, and V. Mbele, Molecular fingerprinting with the resolved modes of a femtosecond laser frequency comb, *Nature* **445**, 627 (2007).
- [12] N. Picqué and T. W. Hänsch, Frequency comb spectroscopy, *Nat. Photonics* **13**, 146 (2019).
- [13] B. Bernhardt, A. Ozawa, P. Jacquet, M. Jacquy, Y. Kobayashi, T. Udem, R. Holzwarth, G. Guelachvili, T. W. Hänsch, and N. Picqué, Cavity-enhanced dual-comb spectroscopy, *Nat. Photonics* **4**, 55 (2009).
- [14] G. Kowzan, D. Charczun, A. Cygan, R. S. Trawiński, D. Lisak, and P. Masłowski, Broadband optical cavity mode measurements at Hz-level precision with a comb-based VIPA spectrometer, *Sci. Rep.* **9**, 1 (2019).
- [15] L. Rutkowski, A. C. Johansson, G. Zhao, T. Hausmaninger, A. Khodabakhsh, O. Axner, and A. Foltynowicz, Sensitive and broadband measurement of dispersion in a cavity using a Fourier transform spectrometer with kHz resolution, *Opt. Express* **25**, 21711 (2017).
- [16] F. C. Roberts, H. J. Lewandowski, B. F. Hobson, and J. H. Lehman, A rapid, spatially dispersive frequency comb spectrograph aimed at gas phase chemical reaction kinetics, *Molecular Physics* **0**, 1 (2020).
- [17] C. Gohle, B. Stein, A. Schliesser, T. Udem, and T. W. Hänsch, Frequency Comb Vernier Spectroscopy for Broadband, High-Resolution, High-Sensitivity Absorption and Dispersion Spectra, *Phys. Rev. Lett.* **99**, 263902 (2007).
- [18] M. C. Stowe, M. J. Thorpe, A. Pe'er, J. Ye, J. E. Stalnaker, V. Gerginov, and S. A. Diddams, Direct frequency comb spectroscopy, *Advances in Atomic, Molecular and Optical Physics* **55**, 1 (2008).
- [19] P. Masłowski, K. F. Lee, A. C. Johansson, A. Khodabakhsh, G. Kowzan, L. Rutkowski, A. A. Mills, C. Mohr, J. Jiang, M. E. Fermann, and A. Foltynowicz, Surpassing the path-limited resolution of Fourier-transform spectrometry with frequency combs, *Phys. Rev. A* **93**, 021802(R) (2016).
- [20] L. Rutkowski, P. Masłowski, A. C. Johansson, A. Khodabakhsh, and A. Foltynowicz, Optical frequency comb Fourier transform spectroscopy with sub-nominal resolution and precision beyond the Voigt profile, *J. Quant. Spectrosc. Radiat. Transfer* **204**, 63 (2018).
- [21] Y.-D. Hsieh, Y. Iyonaga, Y. Sakaguchi, S. Yokoyama, H. Inaba, K. Minoshima, F. Hindle, T. Araki, and T. Yasui, Spectrally interleaved, comb-mode-resolved spectroscopy using swept dual terahertz combs, *Sci. Rep.* **4**, 1 (2014).
- [22] I. Coddington, N. Newbury, and W. Swann, Dual-comb spectroscopy, *Optica* **3**, 414 (2016).
- [23] G. Kowzan, K. F. Lee, M. Borkowski, P. Ablewski, S. Wójtewicz, K. Stec, D. Lisak, M. E. Fermann, R. S. Trawiński, and P. Masłowski, VIPA spectrometer calibration and comb-cavity locking schemes comparison

- for sensitive and accurate frequency comb spectroscopy, *J. Phys. Conf.* **810**, 012035 (2017).
- [24] S. K. Scholten, J. D. Anstie, N. Bourbeau Hébert, R. W. White, J. Genest, and A. N. Luiten, Complex direct comb spectroscopy with a virtually imaged phased array, *Opt. Lett.* **41**, 1277 (2016).
- [25] T. Váczi, A new, simple approximation for the deconvolution of instrumental broadening in spectroscopic band profiles, *Appl. Spectrosc.* **68**, 1274 (2014).
- [26] N. Bourbeau Hébert, S. Scholten, R. White, J. Genest, A. Luiten, and J. Anstie, A quantitative mode-resolved frequency comb spectrometer, *Opt. Express* **23**, 13991 (2015).
- [27] I. E. Gordon, L. S. Rothman, C. Hill, R. V. Kochanov, Y. Tan, P. F. Bernath, M. Birk, V. Boudon, A. Campargue, K. V. Chance, *et al.*, The HITRAN2016 molecular spectroscopic database, *J. Quant. Spectrosc. Radiat. Transfer* **203**, 3 (2017).
- [28] G. Kowzan, K. F. Lee, M. Paradowska, M. Borkowski, P. Ablewski, K. Stec, D. Lisak, M. E. Fermann, R. S. Trawi, and P. Masłowski, VIPA spectrometer for accurate and sensitive self-referenced frequency comb spectroscopy, *CLEO* **2** (2016).
- [29] M. Shirasaki, Large angular dispersion by a virtually imaged phased array and its applications to a wavelength demultiplexer, *Opt. Lett.* **21**, 366 (1996).
- [30] S. K. Scholten, C. Perrella, J. D. Anstie, R. T. White, and A. N. Luiten, Accurate Optical Number Density Measurement of $^{12}\text{CO}_2$ and $^{13}\text{CO}_2$ with Direct Frequency Comb Spectroscopy, *Phys. Rev. Appl.* **12**, 034045 (2019).
- [31] S. K. Scholten, C. Perrella, J. D. Anstie, R. T. White, W. Al-Ashwal, N. B. Hébert, J. Genest, and A. N. Luiten, Number Density Measurements of CO_2 in Real Time with an Optical Frequency Comb for High Accuracy and Precision, *Phys. Rev. Appl.* **9**, 054043 (2018).
- [32] T. Fortier and E. Baumann, 20 years of developments in optical frequency comb technology and applications, *Comms. Phys.* **2**, 153 (2019).
- [33] A. Bartels, C. W. Oates, L. Hollberg, and S. A. Diddams, Stabilization of femtosecond laser frequency combs with subhertz residual linewidths, *Opt. Lett.* **29**, 1081 (2004).
- [34] W. H. Oskay, S. A. Diddams, E. A. Donley, T. M. Fortier, T. P. Heavner, L. Hollberg, W. M. Itano, S. R. Jefferts, M. J. Delaney, K. Kim, F. Levi, T. E. Parker, and J. C. Bergquist, Single-atom optical clock with high accuracy, *Phys. Rev. Lett.* **97**, 020801 (2006).
- [35] W. C. Swann and S. L. Gilbert, Pressure-induced shift and broadening of 1510–1540-nm acetylene wavelength calibration lines, *J. Opt. Soc. Am. B* **17**, 1263 (2000).
- [36] J. Tennyson *et al.*, Recommended isolated-line profile for representing high-resolution spectroscopic transitions (IUPAC Technical Report), *Pure Appl. Chem.* **86**, 1931 (2014).
- [37] N. H. Ngo, N. Ibrahim, X. Landsheere, H. Tran, P. Chelin, M. Schwell, and J.-M. Hartmann, Intensities and shapes of H_2O lines in the near-infrared by tunable diode laser spectroscopy, *J. Quant. Spectrosc. Radiat. Transfer* **113**, 870 (2012).
- [38] V. P. Kochanov, On systematic errors in spectral line parameters retrieved with the Voigt line profile, *J. Quant. Spectrosc. Radiat. Transfer* **113**, 1635 (2012).
- [39] D. Lisak and J. T. Hodges, Low-uncertainty H_2O line intensities for the 930-nm region, *J. Mol. Spectrosc.* **249**, 6 (2008).
- [40] P. Jacquet, J. Mandon, B. Bernhardt, R. Holzwarth, G. Guelachvili, T. W. Hänsch, and N. Picqué, in *Advances in Imaging* (Optical Society of America, Vancouver, Canada, 2009), p. FMB2.
- [41] N. Bourbeau Hébert, V. Michaud-Belleau, S. Magnan-Saucier, J.-D. Deschênes, and J. Genest, Dual-comb spectroscopy with a phase-modulated probe comb for sub-MHz spectral sampling, *Opt. Lett.* **41**, 2282 (2016).
- [42] R. A. Nyquist, *Interpreting Infrared, Raman, and Nuclear Magnetic Resonance Spectra* (Academic Press, United States of America, 2001).
- [43] G. Herzberg, *Molecular Spectra and Molecular Structure: Spectra of Diatomic Molecules* (D. Van Nostrand Company, Prentice-Hall, Princeton, New Jersey, 1950), 2nd ed., Vol. 1.